Chapter 21
Development of an Inverse Identification Method for Identifying Constitutive Parameters by Metaheuristic Optimization Algorithm: Application to Hyperelastic Materials

G. Bastos, A. Tayeb, N. Di Cesare, J.-B. Le Cam, and E. Robin

Abstract In the present study, a numerical method based on a metaheuristic parametric algorithm has been developed to identify the constitutive parameters of hyperelastic models, by using FE simulations and full kinematic field measurements. The full kinematic field was measured at the surface of a cruciform specimen submitted to equibiaxial tension. The test was simulated by using the finite element method (FEM). The constitutive parameters used in the numerical model were modified through the optimization process, for the predicted kinematic field to fit with the experimental one. The cost function was then formulated as the minimization of the difference between these two kinematic fields. The optimization algorithm is an adaptation of the Particle Swarm Optimization algorithm, based on the PageRank algorithm used by the famous search engine Google.

Keywords Inverse identification · Particle swarm optimization · Hyperelasticity · Digital image correlation

Introduction

The constitutive parameters of hyperelastic models are generally identified from three homogeneous tests, basically the uniaxial tension, the pure shear and the equibiaxial tension. From about 10 years, an alternative methodology has been developed [1–4], and consists in performing only one heterogeneous test as long as the field is sufficiently heterogeneous. This is typically the case when a multiaxial loading is applied to a 3 branch [1] or a 4-branch [2] cruciform specimen, which induces a large number of strain states at the specimen surface. The Digital Image Correlation (DIC) technique is generally used to characterize the full kinematic field at the specimen surface. The induced heterogeneity is analysed through the distribution of the biaxiality ratio and the maximal eigen value of the strain. Thus, a large number of experimental data is provided for identifying the constitutive parameters of the considered model.

Several methods have been recently developed to identify parameters from experimental field measurements, typically the finite element updating method (FEMU), the constitutive equation gap (CEGM), the virtual fields method (VFM), the equilibrium gap method (EGM) and the reciprocity gap method (RGM). These methods are fully reviewed in [5].

In the present study a new methodology is proposed in order to minimize the cost function in the FEMU approach. The optimization algorithm used is based on the Particle Swarm Optimization (PSO) algorithm and the artificial smart PageRank algorithm used by the famous search engine Google. This algorithm enables us to the minimize the full kinematic field differences by modifying the constitutive parameters, while minimizing the CPU calculation time. Even though the final objective is the identification of complex constitutive models, i.e. a large number of constitutive parameters, the two-parameter Mooney's model [6] is presented in this paper to illustrate the methodology.

G. Bastos (✉) · A. Tayeb · J.-B. Le Cam · E. Robin
Univ. Rennes 1, CNRS, IPR (Institut de Physique de Rennes), UMR 6251, Rennes, France
e-mail: adel.tayeb@univ-rennes1.fr; jean-benoit.lecam@univ-rennes1.fr; eric.robin@univ-rennes1.fr

N. Di Cesare
Université Bretagne Sud, UMR CNRS 6027, IRDL, Lorient, France
e-mail: noelie.di-cesare@univ-ubs.fr

A. Baldi et al. (eds.), *Residual Stress, Thermomechanics & Infrared Imaging and Inverse Problems, Volume 6*,
Conference Proceedings of the Society for Experimental Mechanics Series, https://doi.org/10.1007/978-3-030-30098-2_21

Experimental Setup

The material considered here is a carbon black filled natural rubber. The specimen geometry is shown in Fig. 21.1. It is a 105 mm long and 2 mm thick cruciform specimen. Figure 21.2 presents an overview of the experimental setup composed of a home-made biaxial testing machine and an optical camera. The machine is composed of four independant RCP4-RA6C-I-56P-4-300-P3-M (IAI) electrical actuators. They were driven by a PCON-CA-56P-I-PLP-2-0 controller and four PCON-CA (IAI) position controllers. The actuators were controlled by an in-house LabVIEW program. Two cell loads, whose capacity is equal to 1094 N, store the force variation in the two perpendicular directions. In the present study, one equibiaxial loading was carried out in such a way that the specimen's centre was motionless for the displacement measurement to be easier. The displacement and loading rate were set at 70 mm and 150 mm/min respectively for the four independent actuators.

Images of the specimen surface at increasing stretches were stored at a frequency equal to 5 Hz with a IDS camera equipped with a 55 mm telecentric objective. The charge-coupled device (CCD) of the camera has 1920 × 1200 joined pixels. The Digital Image Correlation (DIC) technique is used to determine the displacement field at the specimen surface. The software used for the correlation process was SeptD [7], and a uniform cold lighting was ensured by a home-made LED lamp. The spatial resolution, defined as the smallest distance between two independent points was equal to 4 pixels corresponding to 0.343 mm. The Region Od Interest (ROI) used for the digital correlation is represented in Fig. 21.3.

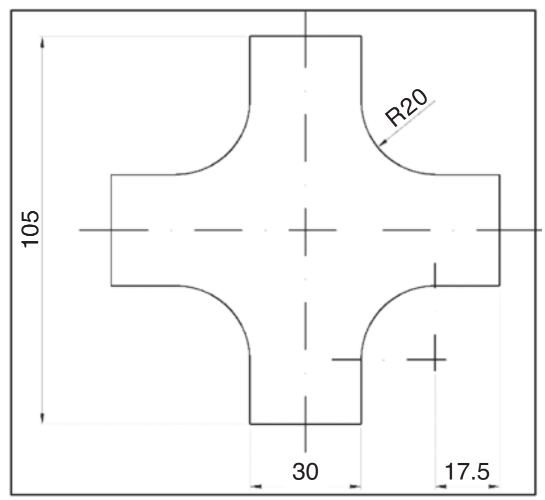

Fig. 21.1 Specimen geometry (dimensions in mm)

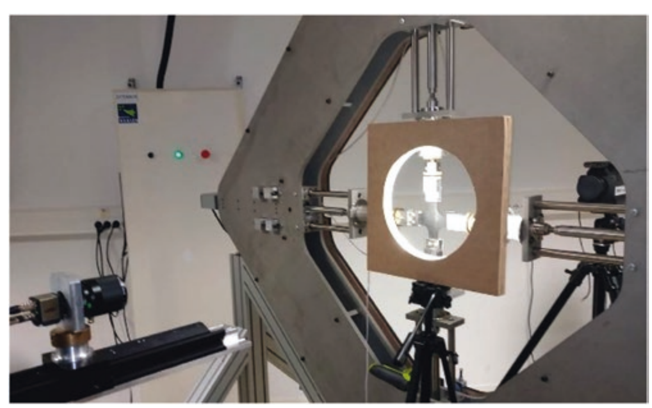

Fig. 21.2 Home-made biaxial testing machine

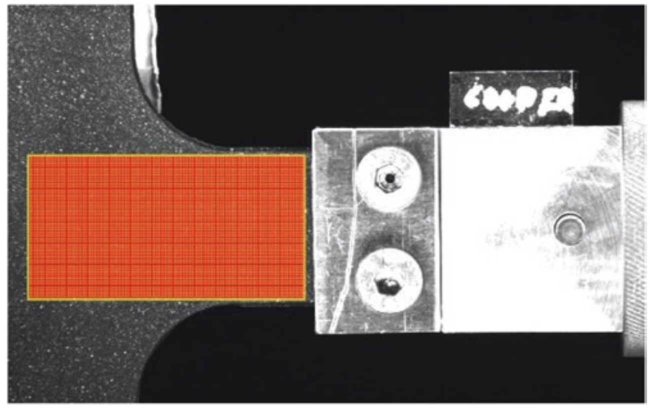

Fig. 21.3 Region of interest for the DIC technique

Numerical Model

A finite element calculation is performed by assuming plane stress state and material incompressibility. The four-node PLANE182 ANSYS element is used. The mesh is made of 9600 nodes, and 9353 elements. A biaxial traction load is obtained by prescribing the same displacement of 70 mm on the four branches of the specimen. The two-parameters hyperelastic Mooney model is used for the calculation. The values of the constitutive parameters are changing at each iteration of the optimization process, as described in the next section.

As the spatial resolution between the predicted and the measured kinematic field was different, the experimental kinematic field was fitted by a polynomial-based function. In this way, the predicted kinematic field was compared, for each node, with the experimental field at the same position of the specimen. With the fitting method applied, the difference between the experimental field and the polynomial-based function was less than 0.2 mm whatever the point considered.

Metaheuristic Optimization Strategy

The aim of the optimization process was here to find the constitutive parameters for the numerical kinematic field to fit the experimental one. The cost function f was the squared difference between the experimental and the numerical fields, considering the force too, as follows:

$$f = min\sum_{i=1}^{N} \frac{1}{N}\left(\frac{U_{x,exp} - U_{x,num}}{U_{x,exp}}\right)^2 + \frac{F_{exp} - F_{num}}{F_{exp}}$$

where N is the number of nodes in the numerical ROI, $U_{x,exp}$ is the polynomial-based experimental displacement, $U_{x,num}$ is the numerical horizontal displacement, F_{exp} is the experimental horizontal force, and F_{num} is the numerical horizontal force.

The optimization algorithm used is an adaptation of the classical Particle Swarm Optimization algorithm. In this version, all the particles are influenced by all the others, by considering this influence to be adapted as a function of the respective performance of the particles. The population of PSO particles is then considered as a Markov chain, in which the particles are the nodes, and the transition probabilities between them are the links between them. For each particle, the PageRank value—that is the steady state of the considered Markov chain—is given by the following equation (2). In this way, the PageRank value of each particle is deduced from its performance compared to the best one.

$$\pi_{target}^{T} = \left| \frac{fitness\left(\boldsymbol{G_{best}}\right)\times 100}{fitness\left(\boldsymbol{G_{best}}\right) - fitness\left(\boldsymbol{P}\right) + \varepsilon} \right|$$

It is then possible to deduce the transition connectivity matrix **C** giving the influence of all the particles on all the others by using a pseudo-random process. The classical equations of PSO are then modified, weighing the influence of all the particles by using the components of **C**, as follow:

$$V_i^{t+1} = \omega \times V_i^t + c_1 \times rand_1 \times \left(P_{i,best}^{t+1} - X_i^t\right) + c_2 \times rand_2 \times \sum\nolimits_{j=1}^{n} C_{ij} \times \left(P_{j,best}^{t+1} - X_i^t\right)$$

$$X_i^{t+1} = X_i^t + V_i^{t+1}$$

where V_i^{t+1} is the speed of the *i*th particle at iteration $t + 1$, c_1 and c_2 are confident parameters, ω is the inertia weight, X_i^{t+1} is the position of particle *i* at iteration $t + 1$, $rand_1$ and $rand_2$ are random numbers given in [0, 1], $P_{j,best}^{t+1}$ is the personal best position of particle *i* at iteration $t + 1$, and C is the transition connectivity matrix of the considered Markov chain. This Inverse-PageRank-PSO algorithm is fully described in [8].

Results and Discussion

As the particles are initially randomly defined, the optimization was launched 10 times, to compare the obtained solutions, and be sure that the global minimum of the cost function was reached. The convergence curves of the 10 launched optimization calculation are represented in Fig. 21.4. The obtained values of the cost function and constitutive parameters are given in Table 21.1.

The validation of the optimized results is checked by comparing the experimental displacements and efforts in the sample with the numerical optimized one. In the final numerical model, the values of the constitutive parameters have been set to the mean of the obtained optimized values found in the 10 different calculations launched. Figure 21.5 shows the difference between the experimental polynomial-based kinematic field, and the optimized numerical one, for every point in the ROI.

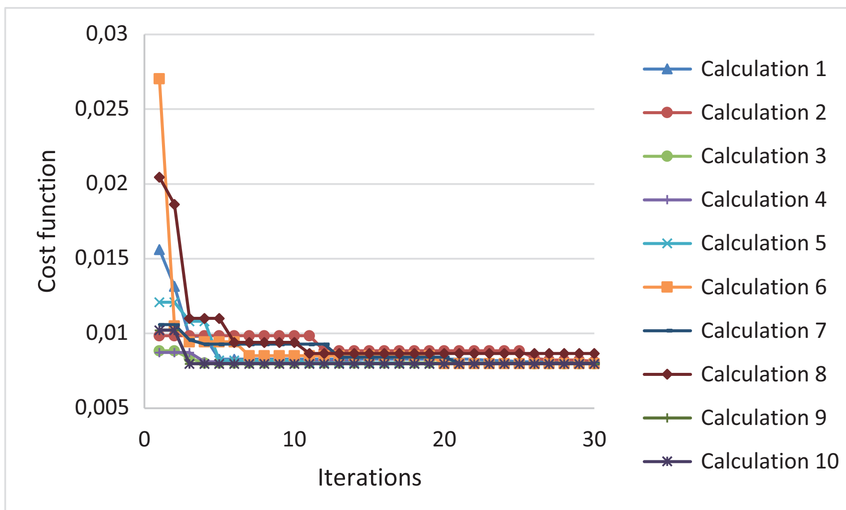

Fig. 21.4 Convergence curves of the 10 optimization calculation launched

Table 21.1 Obtained results

Obtained results			
Optimization number	Cost function	C01	C10
1	8.05×10^{-3}	0.5159	0.01792
2	8.13×10^{-3}	0.5116	0.022541
3	7.98×10^{-3}	0.5188	0.020369
4	7.98×10^{-3}	0.5197	0.018879
5	7.98×10^{-3}	0.5176	0.019914
6	7.99×10^{-3}	0.5175	0.020986
7	8.01×10^{-3}	0.5153	0.02008
8	8.03×10^{-3}	0.5146	0.022146
9	8.15×10^{-3}	0.5109	0.021573
10	7.98×10^{-3}	0.5202	0.019215
Mean	8.03×10^{-3}	5.16×10^{-1}	2.03×10^{-2}
Std	6.475×10^{-5}	3.19×10^{-3}	1.15×10^{-4}

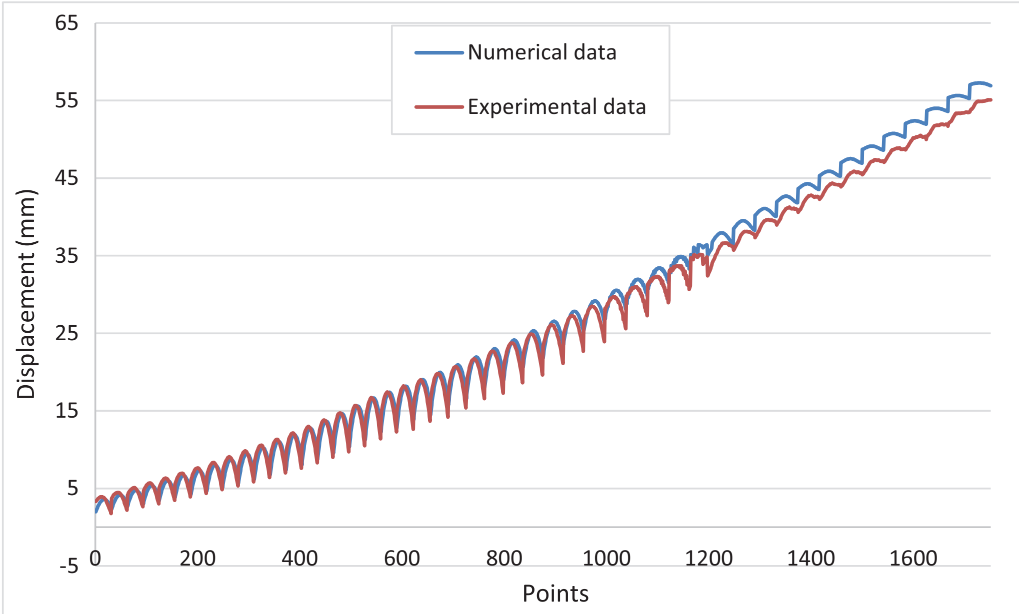

Fig. 21.5 Comparison between the kinematic fields after the optimization process

Fig. 21.6 Difference between the kinematic fields for every point of the ROI

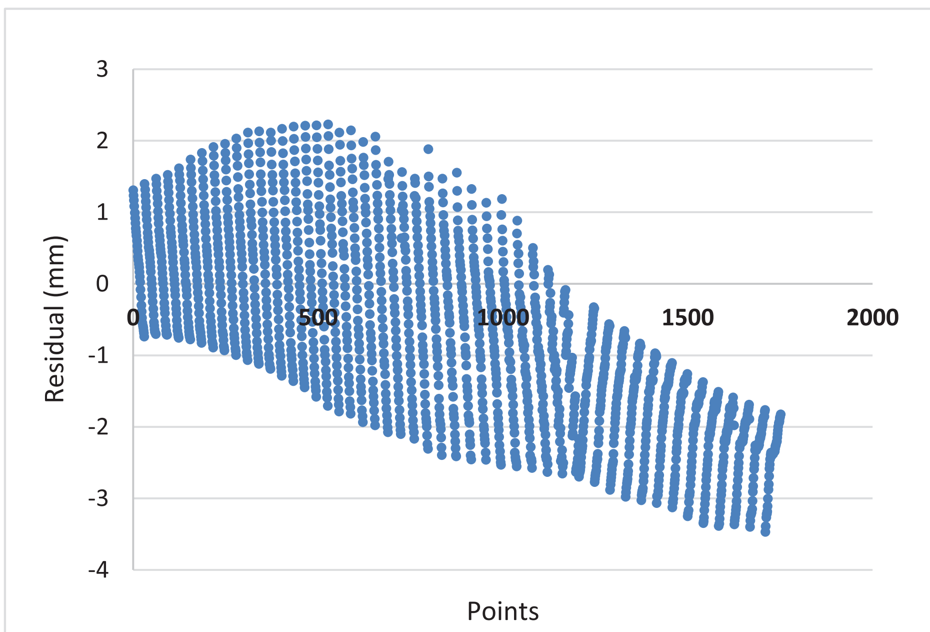

This difference is presented in a quantitative way in Fig. 21.6 showing the difference between the two fields for every point of the ROI. One can note that the difference is always less than 6.5% of the experimental kinematic field. Considering the force, the experimental value was 176.02 N, while the numerical value obtained with the optimized values of the constitutive parameters is 176.37 N, which leads to a difference up to 0.4%.

Conclusions

This work is proposing a new inverse identification method based on the coupling of experimental kinematic fields retrieved by DIC, and the using of a PSO-based parametric optimization algorithm. Experimental and numerical kinematic fields are compared to finally be fitted through the optimization process, while the constitutive parameters are smartly modified.

Applied on a Mooney model, this process is able to find the constitutive parameters reproducing the mechanical response of the specimen, while minimizing the number of optimization iterations. The constitutive parameters found by the optimization process are actually giving a numerical model that retrieves precisely the entire kinematic experimental field.

Acknowledgements The authors thank the Region Bretagne, Rennes Métropole and Université Bretagne Loire for their financial support. Cooper Standard is aknowledged for providing the specimens. Authors also thank Dr. Mathieu Miroir, M. Vincent Burgaud, and M. Mickael Le Fur for having designed the biaxial testing machine, Gilles Marckmann and Prof. Michel Grédiac for the fruitfull discussions.

References

1. T. Guélon, E. Toussaint, J.-B. Le Cam, N. Promma, M. Grédiac, A new characterization method for rubbers. Polym. Test. **28**, 715–723 (2009)
2. N. Promma, B. Raka, M. Grédiac, E. Toussaint, J.-B. Le Cam, X. Balandraud, F. Hild, Application of the virtual fields method to mechanical characterization of elastomeric materials. Int. J. Solids Struct. **46**, 698–715 (2009)
3. M. Johlitz, S. Diebels, Arch. Appl. Mech. **81**, 1333–1349 (2011)
4. H. Seibert, T. Scheffer, S. Diebels, Tech. Mech. **81**, 72–89 (2014)
5. S. Avril, M. Bonnet, A. Bretelle, M. Grédiac, F. Hild, P. Ienny, F. Latourte, D. Lemosse, S. Pagano, S. Pagnacco, F. Pierron, Overview of identification methods of mechanical parameters based on full-field measurements. Exp. Mech. **48**, 381–402 (2008)
6. M. Mooney, A theory of large elastic deformation. J. Appl. Phys. **11**, 582–592 (1940)
7. P. Vacher, S. Dumoulin, F. Morestin, S. Mguil-Touchal, Bidimensional strain measurement using digital images. Proc. Inst. Mech. Eng. C J. Mech. Eng. Sci. **213**, 811 (1999)
8. N. Di Cesare, D. Chamoret, M. Domaszewski, A new hybrid algorithm based on a stochastic Markov chain model. Adv. Eng. Softw. **90**, 127–137 (2015)